LWT - Food Science and Technology 213 (2024) 117046

Contents lists available at ScienceDirect

LWT

journal homepage: www.elsevier.com/locate/lwt

Effect of ultrasonic-pretreatment on soaking kinetics, nutritional, anti-nutritional, and functional properties of guar seeds

Ankan Kheto [a], Aditi Chaudhari [a], Sakshi Manikpuri [a], Rachna Sehrawat [a,*], Khalid Gul [a], Lokesh Kumar [b,**], Khursheed Alam Khan [c]

[a] Department of Food Process Engineering, National Institute of Technology, Rourkela, Odisha, 769008, India
[b] Department of Wine, Food and Molecular Biosciences, Lincoln University, Lincoln, 7647, New Zealand
[c] College of Horticulture, Mandsaur of RVSKVV, Gwalior, Madhya Pradesh, 474002, India

ARTICLE INFO

Keywords:
Anti-nutritional factors
Guar seeds
In-vitro protein digestibility
Multivariate analysis
Soaking
Ultrasound

ABSTRACT

The study aimed to understand how varying the amplitude (25, 50, and 75%) and duration (15, and 30 min) of ultrasonic (US) pretreatment affected the soaking kinetics, nutritional, anti-nutritional factors (ANFs), *in-vitro* protein digestibility, and functional properties of guar seeds (GS). The GS required ~1080 min to hydrate and absorbed ~4.66 times higher moisture content. The US pretreatment reduced ~55.55% of soaking duration compared to control. Soluble protein and fat content was significantly ($p < 0.05$) varied with US-treatment conditions. The water absorption capacity and foaming capacity of GSF samples gradually improved. Expect 75% amplitude, bioactive compounds in GSF begin to rise with longer duration and amplitude than control. Noticeable reduction of ANFs was observed in US-pretreated soaked GSF samples. As observed from FTIR and XRD analysis, US pretreatment might have reorganized structure orientation. Meanwhile, *in-vitro* protein digestibility gradually increased with US amplitude and duration. From multivariant analysis, 75% amplitude-15 min of US pretreatment may be a better option for shorter soaking time, and lesser ANFs. Therefore, US pretreatment could be helpful in increasing the protein extraction yield of GS. Furthermore, US-pretreated soaked GS might be useful to formulate bakery items.

1. Introduction

Guar seeds (GS) belong to the Leguminosae family and are rich in nutrients, bioactive compounds, and anti-nutritional factors (ANFs), restricting their commercial utilization as a food ingredient (Kheto, Behera, et al., 2024). GS is primarily used for guar gum production due to its high galactomannan content (75–85%) in the endosperm portion (Kheto et al., 2023, 2024a; Manikpuri et al., 2024; Prajapati et al., 2013; Salehi et al., 2024). Meanwhile, GS can grow in diverse conditions and requires less water to cultivate. Therefore, cost-effective, energy-efficient, and convenient technology needs to be identified for GS processing.

Soaking is essential step for processing, as it reduces ANFs, softens tissue for further unit operations, and breaks dormancy (Estivi et al., 2022; Kumar et al., 2023). It also helps to isolate starch, protein, and other valuable compounds. Inadequate soaking time may result in sticky slurry after grinding, lowering yield and purity of isolated items (Zhang et al., 2021). Longer soaking times lose nutrients and texture (Zhang et al., 2021). Conventional soaking takes more time to hydrate properly and requires more energy at higher temperatures. The traditional soaking method must be replaced with suitable technology to reduce the overall processing time.

Ultrasonic (US) treatment is widely used in industrial sectors and is recognized as a "green technology" due to its low environmental impact and energy requirements (Eftekhari et al., 2023; Salehi & Inanloodoghouz, 2023). When an US wave passes through a medium, it causes vibrations and the formation of micro-bubbles (Abi-Khattar et al., 2022). Then, newly formed micro-bubbles rapidly expand to reach the critical limit (i.e., double in size) before collapsing (Chemat et al., 2017). Then, ultrasound induced acoustic cavitation generates microturbulence collapsed micro-bubbles and increases shear stress (up to 50 MPa), temperature (up to 5000 K), and pressure in the medium (Abi-Khattar et al., 2022; Chemat et al., 2017; Eftekhari et al., 2023; Kumar et al., 2023; Zhang et al., 2021). As a result, the treated samples showed

* Corresponding author.
** Corresponding author.
E-mail addresses: sehrawatrachna2017@gmail.com, sehrawatr@nitrkl.ac.in (R. Sehrawat), Lokesh.Kumar@lincoln.ac.nz (L. Kumar).

https://doi.org/10.1016/j.lwt.2024.117046
Received 6 February 2024; Received in revised form 3 November 2024; Accepted 11 November 2024
Available online 13 November 2024

structural orientation changes as well as biochemical changes such as the breakdown of intermolecular bonds, the formation of free radicals, polymerization, and macromolecule denaturation (Abi-Khattar et al., 2022; Zhang et al., 2021). However, cavitation bubbles and surface area are the primary causes of subsequent changes in the food matrix (Abi-Khattar et al., 2022). Meanwhile, ultrasound treatment accelerates mass transfer and improves diffusion rates by degrading cell matrixes and increasing surface area (Abi-Khattar et al., 2022; Eftekhari et al., 2023; Zhang et al., 2021). Additionally, increase in US intensity has noticeably enhanced the acoustic cavitation and sponge effect, which will ultimately affect the moisture migration rate on treated samples (Salehi, 2023; Salehi & Inanloodoghouz, 2023).

The US technology was frequently used to extract bioactive compounds and modifies starch and protein. Previously, US pretreatment was carried out on corn, sorghum, andean lupin, durum wheat, and pantanal rice, which focused primarily on the soaking kinetics and mass transfer rate (Aires et al., 2023; Miano et al., 2017, 2019; Patero & Augusto, 2015; Yıldırım, 2022). Similarly, Pacheco et al. (2024) reported that US-pretreatment could reduce 54.3% of pumpkin seed soaking duration and have a positive impact on germination process. Meanwhile, the effects of US-pretreated soaked grain on ANFs and bioactive compounds have not been thoroughly investigated. To the best of our knowledge, no research has been carried out regarding the effects of US-pretreated soaking on GS physicochemical properties. However, the increasing demand for gluten-free ingredients with higher nutritional properties has become a major concern. As a result, the effect of US-pretreated soaked GS on bioactive compounds, ANFs, and *in-vitro* protein digestibility (*IVPD*) is critical when developing bakery items. Therefore, the current study was intended to investigate the effects of varying US amplitude and duration on soaking kinetics, nutritional and bioactive compounds, ANFs, functional properties, and *IVPD* in GS samples. In addition, statistical correlations between treatment conditions and analyzed parameters were visualized using person correlation analysis, principal component analysis, and hierarchical clustering analysis. The study will also help to identify the potential applications of US technology for ANFs-rich legumes. Formulating bakery items using US-pretreated soaked GS may be a better option for fulfilling market demand while maintaining nutritional value.

2. Material and methods

2.1. Raw material

Matured GS (GEETA-51) was purchased from a local market in Rourkela, India. Following that, the samples were manually cleaned and sorted based on size. Then, uniform GS was chosen for further investigation.

2.2. Ultrasonic pretreatment and soaking process

Initially, 10 g of GS was placed in a beaker containing 75 mL of distilled water (DW). For US pretreatment, the sample was placed in a probe US sonicator (Qsonica sonicators, Newtown, USA) with an amplitude of 25–75% and a pulse on/off time of 5 s, as per the reported methodology of Yadav et al. (2021). However, US pretreatment was carried out for 15 and 30 min at a maximum power of 700 W and a frequency of 20 kHz, respectively. The control and US-pretreated GS were kept in a water bath at 25 °C. The hydrated GS's weight was measured every 30 min for the first 2 h, then every 60 min for the next 2–6 h, and finally every 120 min until it reached a constant weight. Meanwhile, GS was gently wiped with tissue paper to remove any excess surface water before weighing. In addition, GS's moisture content (dry basis) was determined using a hot air oven (105 °C). The hydration behaviour of GS was investigated in triplicate.

2.3. Mathematical modelling

The hydration kinetics of control and US-pretreated GS were fitted with the Peleg model (Kalita et al., 2021) using Eq. (1).

$$M_t = M_o + \frac{t}{K_1 + K_1 t} \tag{1}$$

Where: M_o -Initial moisture content (g water/100 g dry matter); M_t - Moisture content at time t (g water/100 g dry matter); K_1 and K_2- rate constants; t-time (min).

The fitting quality of Peleg model was evaluated based on the coefficient of determination (R^2), Chi-square value (χ^2) and residual sum of squares (RSS).

$$\chi^2 = \sum_{i=1}^{N} \frac{\left[(Observed\ value - Expected\ value)^2\right]}{(N-n)}$$

Where: N- number of data point; n-number of unknown coefficients in the Peleg model.

2.4. Hardness

The hardness of control and US-pretreated soaked GS samples was measured using a texture analyzer (TA-XT2, Brookfield, USA) and a 5 N load cell. Throughout the experiment, the probe velocity was kept at 1 mm/s with a compression ratio of 70%. However, the hardness value was measured using a cylinder probe.

2.5. Estimation of carbohydrate, soluble protein and fat contents

The carbohydrate, soluble protein, and fat contents of the samples were determined using the previously described methodology of Kheto et al. (2023). The GS samples were dried in a hot air dryer at 40 °C until the moisture content reached around 16% (dry basis). The dried GS was ground into flour and passed through a 210 μm sieve. The obtained guar seed flour (GSF) was then analyzed for the remaining properties before being packaged in an aluminium pouch for future use. For carbohydrate, the phenol-sulphuric acid method was used. Initially, 70% of sulphuric acid (50 mL) was mixed with sample (500 mg) and carefully mixed for 10 min. After adding 50 mL of DW to the above suspension, incubation was carried out in a water bath for 60 min at 70 °C. After cooled to ambient temperature, filtration (using Whatman No. 3) was performed to collect the supernatant. Then, DW (49.5 mL) and supernatant (0.5 mL) were mixed together, followed by addition of 1 mL phenol solution (5% w/v) and 5 mL concentrated sulphuric acid. After carefully mixing the above solution, the absorbance value was recorded at 480 nm using a UV spectrometer (AU 2701, Systronics India Ltd.), and glucose was used for the preparation of a standard curve. Meanwhile, the modified Lowry method and Soxhlet apparatus were used to determine the soluble protein and fat content, respectively.

2.6. Functional properties

The functional properties (Water absorption capacity (WAC), oil absorption capacity (OAC), water solubility index (WSI), foaming capacity (FC), and emulsifying capacity (EC)) were determined using the method described by Kheto et al. (2023). In WAC, DW (15 mL) was added to sample (1 g) and properly mixed, vortexed (5 min), and then incubated (30 min). Then, centrifugation was carried out for 30 min at 5000 rpm, and discard the supernatant. For OAC, soybean oil was mixed with sample (600 mg) and properly mixed, vortexed (5 min), and then incubated (30 min). After that, centrifugation was carried out for 30 min at 7500 rpm, and discard the supernatant. The WAC/OAC of the samples were determined using Eq. (2).

$$WAC/OAC\left(\frac{g}{g}\right)=\frac{Sample\ weight\ after\ centrifugation-initial\ sample\ weight}{Initial\ sample\ weight} \tag{2}$$

For WSI, DW (10 mL) was added to sample (250 mg) and properly mixed, vortexed (2 min), and then incubated for 30 min at 85 °C. After immediate cooling, centrifugation was carried out at 6000 rpm for 15 min to collect the supernatant and dried for 3 h at 105 °C. The WSI was determined using Eq. (3).

$$WSI\left(\frac{g}{100\ g}\right)=\frac{Final\ weight\ supernatant\ after\ drying}{Initial\ sample\ weight} \tag{3}$$

In FC, DW (50 mL) was mixed with sample (1 g) and vigorously shaken using a hand blender for 5 min. Then, immediately transfer in a measuring cylinder and note down the foam volume. The FC of the sample was determined using Eq. (4).

$$FC\ (\%)=\frac{Foam\ volume}{Initial\ suspension\ volume} \tag{4}$$

For EC, equal volumes of DW and soybean oil (5 mL each) were mixed with the sample (50 mg), properly mixed, vortexed (5 min), and then centrifuged for 5 min (8000 rpm). The suspension was then carefully transferred into a measuring cylinder, and the emulsion volume was measured. Finally, EC of the sample was determined using Eq. (5).

$$EC\ (\%)=\frac{Emulsion\ volume}{Total\ volume} \tag{5}$$

2.7. Bioactive compounds

The bioactive compounds (total phenolic content (TPC), total flavonoid content (TFC), and antioxidant activity (AOA) of control and US-pretreated soaked GSF were determined using our previously reported methodology of Kheto et al. (2023). The Folin-Ciocalteu and aluminum chloride colorimetric assays were used to determine the TPC (mg gallic acid equivalent (GAE) per 100 g) and TFC (mg quercetin equivalent (QE) per 100 g). Similarly, the 1,1-diphenyl-2-picrylhydrazyl colorimetric assay was used to measure AOA. At first, sample (600 mg) was mixed with 15 mL of methanolic solution (80%) and then incubated in a rotary shaker for 60 min at 50 °C. To collect supernatant, centrifugation was carried out for 20 min at 7000 rpm. In TPC, supernatant (100 μL), 10% of FC reagent (2.5 mL), and 7.5% of sodium carbonate (2 mL) were taken in a test tube. After incubating the above solution at 45 °C for 40 min, absorbance value was measured at 765 nm using a UV-spectrometer (AU 2701, Systronics India Ltd.), and methanol was used as a blank. For TFC, supernatant (2 mL) and 10% of aluminum chloride (2 mL) were carefully mixed, vortexed, and then incubated at room temperature for 15 min. After that, absorbance value was measured at 510 nm using a UV-spectrometer (AU 2701, Systronics India Ltd.), and methanol was used as a blank. In AOA, supernatant (100 μL) was mixed with 6×10^{-5} mol/L of DPPH solution (3.9 mL) and incubated in a dark environment for 30 min. Then, absorbance value was measured at 515 nm using a UV-spectrometer (AU 2701, Systronics India Ltd.), and methanol was used as a blank. Finally, the AOA of the sample was calculated using Eq. (6).

$$AOA=\left(1-\frac{\text{Absorbance value of sample}}{\text{Absorbance value of control}}\right)\times 100 \tag{6}$$

2.8. Anti-nutritional factors

The anti-nutritional factors of control and US-pretreated soaked GSF samples were determined according to our previously reported methodology of Manikpuri et al. (2023). For tannin content, the sample (0.5 g) was mixed with 5 mL of acidified methanol (0.5 mL HCl in 50 mL methanol) and incubated (15 h). Further, the sample extract was collected after centrifugation (7000 rpm, 15 min). On the other hand, vanillin-HCl reagent was prepared by mixing vanillin solution (vanillin: methanol: 1: 25) with HCl-methanol solution (4 mL HCl/50 mL methanol) in equal quantity. Then, the solution of extract (0.5 mL) and vanillin-HCl reagent (2.5 mL) was prepared and kept in dark for 20 min. Later, the absorbance value was recorded with a UV- spectrometer (AU 2701, Systronics India Ltd) at 500 nm. The tannic acid was used as standard and represented as mg tannic acid/100 g. To determine phytic acid content, 0.5 g of sample was added to 5 mL of HCl solution (0.2 N), followed by incubation (1 h) and centrifugation (5000 rpm, 15 min) to collect the extract. Then, a solution of extract (0.5 mL) and 1 mL ammonium ferric sulfate (50 mg ammonium ferric sulfate/25 mL HCl (0.2 N)/225 mL DW) was prepared and boiled (30 min). Further, the solution was rapidly cooled and mixed with 2 mL Bipyridine solution (mixture of (1 g Bipyridine, 1 mL thioglycolic acid, 99 mL DW). After incubation for 2 min, a UV-spectrometer (AU 2701, Systronics India Ltd) was used to record the absorbance value at 519 nm with phytic acid as standard and expressed as mg phytic acid/100 g. The saponin content was estimated by mixing sample (0.5 g) with methanol (5 mL) and incubating for 12 h. Later, the extract (1 mL) was added to 10 mL of vanillin (0.8 g vanillin/10 mL ethanol) and H_2SO_4 solution (10 mL). Then, the solution was heated (60 °C, 10 min) and instantly cooled. Finally, the absorbance value was measured at 540 nm through a UV-spectrometer (AU 2701, Systronics India Ltd) with diosgenin as standard and expressed as mg diosgenin/100 g.

2.9. Functional groups

The functional groups of control and US-pretreated GSF samples were analyzed with a Fourier Transform Infrared (FTIR) spectrometer (Alpha E, Bruker, UK), as described by Manikpuri et al. (2023).

2.10. XRD

The X-ray diffraction (XRD) patterns of the control and US-pretreated GSF samples were determined with an X-ray diffractometer (XRD, D8 Advance A25, Brucker, Germany). The relative intensity of the diffraction peak was recorded in the scattering range (2θ) of 10–50° at a scanning rate of 2°/min with 0.02 steps.

2.11. In-vitro protein digestibility

In-vitro protein digestibility (*IVPD*) of control and US-pretreated soaked GSF samples were measured using a multi-enzyme mixture, as previously reported by Manikpuri et al. (2023). Initially, 50 mL of suspension (sample: DW = 1:1) was prepared by adding DW. The pH of the suspension was then adjusted to 8 through 0.1 N of alkaline (sodium hydroxide) or acid (hydrochloric acid) solution and incubated at 37 °C under continuous shaking. Meanwhile, multienzymes such as trypsin (8 mg), α-chymotrypsin (15.5 mg), and peptidase (6.5 mg) were mixed with 5 mL of DW. Finally, 5 mL of enzyme solution was carefully added to above suspension and measured the pH after 10 min. However, *IVPD* of the sample was calculated using Eq. (7).

$$IVPD=210.46-18.103z \tag{7}$$

Where z indicates the suspension pH.

2.12. Statistical analysis

All analyses have been carried out in triplicate and reported as mean ± SD. The Origin Pro (2018) software (version 9.50.0, Northampton, USA) was used for mathematical modelling, person correlation analysis, principal component analysis, and hierarchical clustering analysis. However, one-way ANOVA with Duncan's multiple range test was performed using IBM SPSS software (Version 25.0, Chicago, IL).

3. Results and discussion

3.1. Soaking kinetics of guar seeds

The hydration behaviour of GS followed a downward concave shape (Fig. 1), similar to other grains (Lee et al., 2023; Miano et al., 2017). During initial soaking phase, GS rapidly absorbed water molecules through intercellular pores, as induced by capillary action and higher concentration gradient difference. In the meantime, water molecules diffuse from internal core (germ) to outer layer (through the endosperm) of GS. After 90 min of hydration, water absorption rate declined over time and ultimately reached saturated moisture content (MC) (~67.29% w.b). Compared to other grains, untreated GS required ~1080 min to reach saturated MC, indicating a slow hydration process (Kalita et al., 2021; Miano et al., 2017). Interestingly, soaked GS samples absorbed ~4.66 times more MC than initial. The present finding coincides with a previous study by Miano et al. (2017) for maize (4.5-fold higher MC). According to the literature, hydration behaviour of any grain depends on seed coat thickness, compactness, compositions, and internal structure (Estivi et al., 2022; Kalita et al., 2021). Meanwhile, legumes required much more time to reach saturated MC due to the thick and compact arrangement of starch granules, particularly in the endosperm, and lignin on cotyledon cells, which eventually hinders water penetration rate (Perera et al., 2023).

Among different legumes, GS processed the longest soaking duration due to its compositions (starch (25.2–59.1%), protein (24.55–35%), and galactomannan) and unique structural components (13–18% of hull, 34–43% of endosperm, and up to 46% of germ) (Kheto et al., 2023; Prajapati et al., 2013). Furthermore, endosperm portions contained 75–85% galactomannan and slowly hydrated to become soluble (Prajapati et al., 2013). The US-pretreated GS samples had a higher moisture absorption capacity and were positively correlated with treatment duration and amplitude. An increase in US amplitude/duration considerably decreased the overall soaking time from 900 to 600 min. Most importantly, US pretreatment reduced ~55.55% of soaking duration compared to control. Therefore, US pretreatment might be helpful to reduce the overall processing time for GS.

The faster soaking process of US-pretreated samples could be attributed to several factors, including i) strong shear forces due to cavitation phenomena and ii) bubbles collapsing specifically at the outer layer. As a result, covalent and ionic bonds can be destroyed in cell walls, weakening the cellular matrix and forming porous structures in the hilum and micropyle. Also, it can form micro-jets and surface etching at the outer layer, leading to microchannels and nanopores that extend into the inner regions, increasing the mass transfer rate (Estivi et al., 2022; Kumar et al., 2023). Furthermore, the cell matrix expanded and contracted rapidly, resulting in faster water molecule penetration and diffusion than control (Abi-Khattar et al., 2022; Kumar et al., 2023). Higher amplitude/duration US pretreatment, on the other hand, can cause fragmentation within the cellular matrix, which causes smooth connections between microchannels and eventually increases the diffusion rate (Abi-Khattar et al., 2022; Kumar et al., 2023).

Table 1 shows the hydration kinetics of control and US-pretreated GS at 25 °C using the Peleg model and determined the coefficient of determination (R^2), chi-square (χ^2), and residual sum of squares (RSS). In the Peleg model, K_1 and K_2 represent the mass transfer rate and water absorption capacity, respectively (Pramiu et al., 2015). The control sample exhibited a higher mass transfer rate than the others. However, lower K_1 indicates rapid moisture absorption, as observed in US-pretreated samples. It could be related to the formation of microchannels and degradation of cell wall weakness, as induced by cavitation and sponge effect, resulting in faster water penetration rate. The R^2 value for all samples was greater than 0.9, indicating that the Peleg model was well-fitted. χ^2 values were also near zero. The RSS value, on the other hand, decreased gradually as the amplitude and duration increased. Based on the results, the Peleg model was found to be suitable for understanding GS soaking kinetics. Pramiu et al. (2015) and Kalita et al. (2021) reported that the Peleg model was appropriate to explain the hydration behaviour of low-pressure treated chickpeas and US-pretreated paddy.

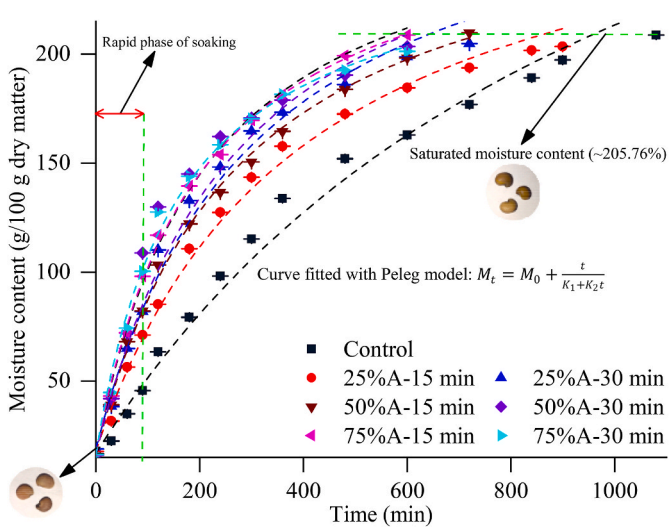

Fig. 1. Effect of US pretreatment on soaking kinetics of guar seeds.

3.2. Hardness

The hardness of US-pretreated soaked GS was slightly lower than the control but not significantly ($p < 0.05$) different (Table 2). A minor reduction in hardness may be associated with higher cell permeability due to middle lamella degradation (Zhang et al., 2021). Meanwhile, cavitation can form macropores and microchannels throughout cell matrixes, reducing hardness (Abi-Khattar et al., 2022). Furthermore, higher amplitude and duration of US pretreatment could have generated strong shear stress and mechanical vibrations on GS, resulting in loss of structural integrity (Chemat et al., 2017; Kumar et al., 2023). Lee et al. (2023) reported that US-pretreated soaked adzuki became softer than control. However, a non-significant ($p < 0.05$) difference in hardness might be associated with the structural composition of GS. Most importantly, soaked GS almost reached 7.15 times its initial volume. Whereas hull and endosperm fractions comprised around 76.3% of total volume in soaked GS. Furthermore, endosperms rich in galactomannan could have played an important role in the hardness of soaked GS.

3.3. Carbohydrate, soluble protein and fat content

The carbohydrate, soluble protein, and fat content in control and US-pretreated soaked GSF samples are shown in Table 2. No significant ($p < 0.05$) difference in carbohydrate content was observed in US-pretreated samples. These phenomena might be related to cavitation phenomena, which may destroy longer glucose chains and weaker interactions and

Table 1
Peleg model constants of US-pretreated soaked guar seeds.

Amplitude (%)	Control	25		50		75	
Time (min)	–	15	30	15	30	15	30
K_1	2.636	1.417	1.083	1.033	0.798	0.774	0.68
K_2	0.002	0.003	0.003	0.003	0.003	0.003	0.004
R^2	0.983	0.993	0.991	0.997	0.987	0.999	0.993
χ^2	0.008	0.003	0.004	0.001	0.008	0.006	0.025
RSS	0.112	0.046	0.047	0.016	0.071	0.057	0.023

Where, K_1 and K_2: rate constants, R^2: coefficient of determination, RSS: residue sum of square, and χ^2: reduced chi square.

Table 2
Effect of US-pretreated soaking on hardness, carbohydrate, soluble protein, fat, and functional properties of guar seeds.

Amplitude (%)	Time (min)	Hardness (N)	Carbohydrate (%)	Soluble protein (%)	Fat (%)	WAC (g/g)	OAC (g/g)	WSI (g/100 g)	FC (%)	EC (%)
Control	0	16.09 ± 0.58^{a}	56.58 ± 0.09^{a}	26.49 ± 0.08^{c}	3.61 ± 0.07^{a}	2.17 ± 0.09^{a}	1.29 ± 0.08^{a}	25.41 ± 0.09^{a}	110.97 ± 1.46^{a}	39.81 ± 0.09^{a}
25	15	15.98 ± 0.37^{a}	56.75 ± 0.18^{a}	26.65 ± 0.09^{bc}	3.65 ± 0.03^{ab}	2.21 ± 0.01^{a}	1.26 ± 0.03^{ab}	24.95 ± 0.05^{b}	115.55 ± 0.93^{b}	39.16 ± 0.05^{b}
	30	15.87 ± 0.25^{a}	56.89 ± 0.12^{a}	26.95 ± 0.11^{ab}	3.72 ± 0.05^{abc}	2.38 ± 0.07^{bc}	1.19 ± 0.06^{abc}	23.84 ± 0.03^{c}	127.68 ± 1.06^{c}	37.96 ± 0.04^{c}
50	15	15.95 ± 0.2^{a}	56.83 ± 0.11^{a}	27.05 ± 0.13^{a}	3.68 ± 0.04^{abc}	2.29 ± 0.03^{ab}	1.22 ± 0.04^{abc}	24.22 ± 0.06^{d}	120.29 ± 1.38^{d}	38.55 ± 0.02^{d}
	30	15.71 ± 0.16^{a}	57.01 ± 0.14^{a}	27.18 ± 0.07^{a}	3.77 ± 0.05^{cd}	2.41 ± 0.04^{bce}	1.15 ± 0.03^{bc}	23.52 ± 0.02^{e}	132.56 ± 1.16^{e}	36.73 ± 0.03^{e}
75	15	15.62 ± 0.24^{a}	56.94 ± 0.13^{a}	27.09 ± 0.06^{a}	3.74 ± 0.01^{bcd}	2.48 ± 0.02^{cd}	1.20 ± 0.02^{abc}	23.76 ± 0.07^{c}	124.63 ± 0.93^{f}	37.46 ± 0.02^{f}
	30	15.45 ± 0.19^{a}	56.99 ± 0.16^{a}	26.89 ± 0.08^{ab}	3.83 ± 0.02^{d}	2.54 ± 0.03^{d}	1.13 ± 0.01^{c}	23.15 ± 0.01^{f}	119.64 ± 0.96^{d}	36.34 ± 0.01^{g}

Values are means ± standard deviations (n = 3). The superscripts a, b, c, d, e, f and g represent significant ($p < 0.05$) effect of ultrasound-assisted soaking on guar seeds. WAC: Water Absorption Capacity (g/g), OAC: Oil Absorption Capacity (g/g), WSI: Water solubility index (g/100 g), FC: Foaming Capacity (%) and EC: Emulsifying Capacity (%).

then organize them in a more ordered structure (Estivi et al., 2022). On the other hand, soluble protein and fat content were significantly ($p < 0.05$) varied with treatment conditions. However, soluble protein content was increased from 26.49 to 27.18% (50%A-30 min) due to the breakdown of intermolecular bonds and ultimately improved the extractability of soluble protein fractions (Zhang et al., 2021). The fat content was also increased from 3.61 to 3.83% (75%A-30 min), which might be responsible for the degradation of the longer fatty acid chain. Meanwhile, lower amplitude and treatment duration may not be able to break the intermolecular interactions between macromolecules. Apart from this, longer soaking duration and excessive degradation of cellular structures can accelerate the leaching of soluble fractions (Zhang et al., 2021). In contrast, Shah et al. (2023) reported that US-pretreated (with varying amplitude and time) paddy did not show any noticeable changes in protein content, which may be responsible for the structural compositions. They also observed that US pretreatment may destroy the side chain of amylopectin and increase the amylose content.

3.4. Functional properties

The functional properties provide an overview of textural, nutritional, and organoleptic properties of processed food items. Soaked GSF showed higher WAC (1.89–2.17 g/g), OAC (1.18–1.29 g/g), and WSI (20.6–25.41 g/100g) than unsoaked samples (Kheto et al., 2023). In WAC, hydrophilic sites of amino acids, protein structure, and carbohydrate content are the major responsible factors in any sample. The WAC of US-pretreated soaked GSF samples gradually improved with amplitude and treatment duration (Table 2). It might be correlated with the better hydrophilic ability of macromolecules due to the destruction of hydrogen bonds and helical structure in starch granules. Likewise, OAC of US-pretreated soaked GSF samples followed a similar trend. These phenomena might be associated with protein unfolding and exposure of polar side chains. In other words, strong shear force, microturbulence, and pressure on GS may lead to exposed hydrophilic and hydrophobic sites. As a result, US-pretreated samples could bind more water/oil with newly exposed sites, eventually increasing the WAC and OAC. In contrast, WSI of GSF samples was significantly ($p < 0.05$) reduced with treatment conditions. The US pretreatment could have induced the cleave formation in a glycosidic bond and depolymerized it into smaller chains with an organized structure (Kumar et al., 2023). In addition, loosely packed granules after US pretreatment might have leached out in prolonged soaking duration of GS and eventually reduced WSI. The results of XRD analysis also supported the present findings. Like others, FC and EC of US-pretreated soaked GSF samples were significantly ($p < 0.05$) varied with treatment conditions. It might be due to the protein unfolding as induced by cavitation and reducing the surface tension of the air and water interface, indicating a higher FC (Kumar et al., 2023). Meanwhile, excessive degradation of macromolecules and then reorganized to order structures may be responsible for reduction in functional properties.

3.5. Bioactive compounds

The bioactive compounds in control and US-pretreated soaked GSF samples significantly ($p < 0.05$) varied (Fig. 2). In comparison with our previous study, soaking process reduced the TPC and TFC of GSF from 521.29 to 460.41 (mg GAE/100 g) and 232.46 to 161.43 (mg QE/100 g), respectively (Kheto et al., 2023). The US-pretreated soaked GSF samples had higher TPC, TFC, and AOA than control. However, bioactive compounds increased with longer duration and/or amplitude (expect 75% A). Furthermore, the highest TPC, TFC, and AOA were observed in the 50%A for 30 min treated GSF sample. It might be associated with cell-matrix fragmentation due to mechanical vibrations and direct contact with microjet. As a result, intermolecular bonds weaken, releasing bound polyphenols (Abi-Khattar et al., 2022). In addition, finely ground samples with a weaker cell matrix might have solubilized the more bioactive compounds in the aqueous solvent. Moreover, structural degradation of macromolecules can expose hydroxyl groups on the outer surface, eventually increasing the bioactive compounds, particularly AOA. On the other hand, high-intensity US pretreatment with a longer duration leads to excessive degradation of the cellular matrix, which may increase the fluidity of the cell walls and result in leaching of water-soluble polyphenols (Abi-Khattar et al., 2022; Cui & Zhu, 2020). Meanwhile, collapse of microbubbles also produced a reactive zone with free radicals (Chemat et al., 2017). Higher US amplitude or duration may accelerate the cavitation phenomenon and accumulate more free radicals. As a result, hydroxyl radicals can rapidly oxidize polyphenols and reduce bioactive compounds (Cui & Zhu, 2020). Additionally, oxidation of polyunsaturated fatty acids might have occurred, resulting in a hydroxylation reaction and reducing the stability of polyphenol compounds (Perera et al., 2023). The present observation was supported by Cui and Zhu (2020) for US-treated sweet potato and wheat flour. They also suggested that high-intensity US treatment may facilitate pyrolysis reactions and degrade the bioactive compounds.

3.6. Anti-nutritional factors

The ANFs of control and US-pretreated soaked GSF varied significantly ($p < 0.05$), as shown in Fig. 2. Soaking process reduced the

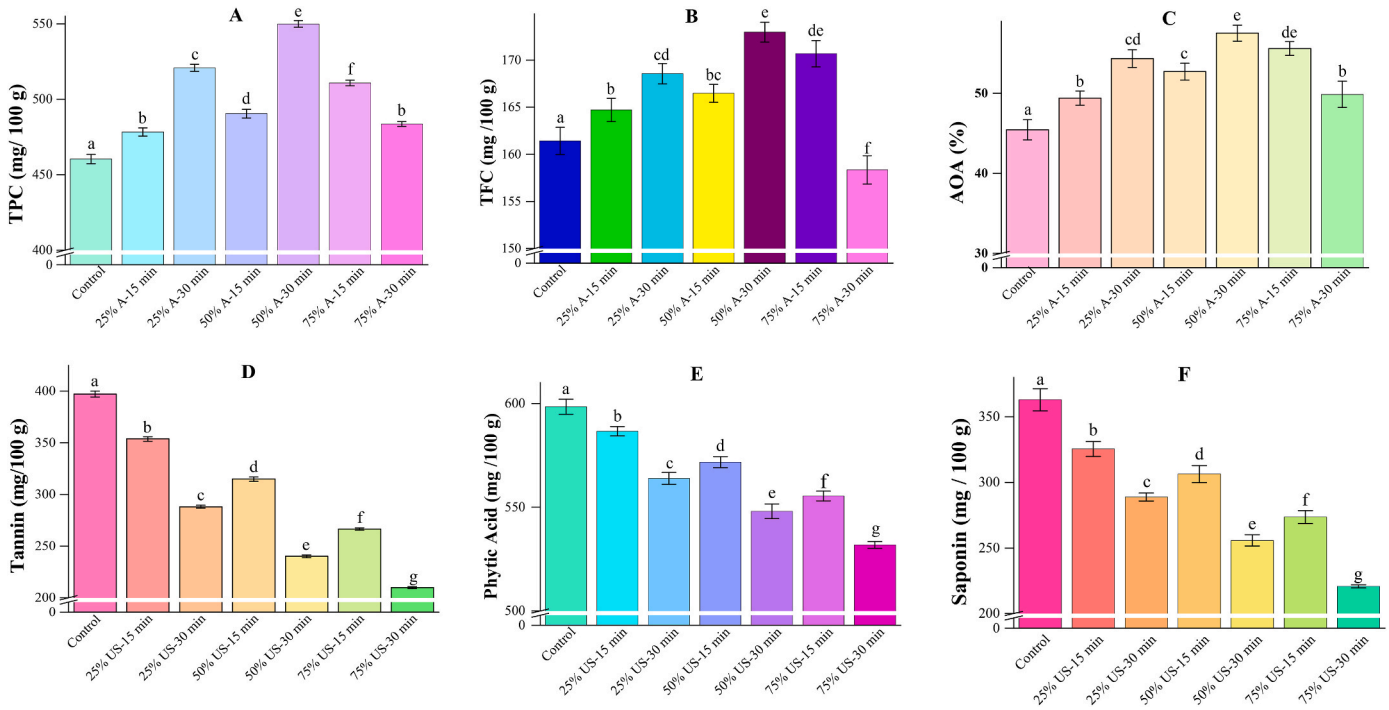

Fig. 2. Effect of US-pretreated soaking on (A) TPC: Total phenolic content (mg GAE/100 g), (B) TFC: Total flavonoid content (mg QE/100 g), (C) AOA: Antioxidant activity (%), (D) Tannin (mg TA/100 g), (E) Phytic Acid (mg phytate/100 g), and (F) Saponin (mg diosgenin/100 g) of guar seed flour.

tannin, phytic acid, and saponin content in GSF than the unsoaked sample from 432.26 to 397.09 (mg TA/100 g), 609.44 to 598.37 (mg phytate/100 g), and 3.97 to 3.63 (mg diosgenin/g), respectively (Kheto et al., 2023). It might be due to the leaching of water-soluble ANFs in soaked samples. The water-soluble nature of tannin might be responsible for hydrolyzable tannin, hydroxyl groups, and ester bond hydrolysis (Yadav et al., 2021). Similarly, phytic acid is rich in hydroxyl groups and phosphates (Sarkhel & Roy, 2022). The increased moisture content may have activated phytase enzymes, leading to the hydrolysis of phytic acid and its eventual degradation. For saponin, hydrolysis in sugar chains and aglycone chains may occur, during the soaking process. However, numerous studies claimed the soaking process had noticeably reduced the ANFs in millets, pluses, and legumes. Unfortunately, the present study showed no drastic changes in ANFs, which might be correlated with the compositions, seed coat thickness, and slow water penetration rate. In GS (after fully hydrated), ~23.7% of its volume was only occupied by germ fractions than hull and endosperm portions, which restrict leaching of water-soluble ANFs.

The US-pretreated soaked GSF samples drastically reduced the ANFs. The US treatment may induce cavitation and produce microjets, microchannels, and strong shear force. In other words, higher amplitude of US treatment accelerated the cavitation phenomena. As a result, stronger interactions (such as –OH and –COOH) with other macromolecules in tannin may have weakened and leached out into water. Meanwhile, newly formed reactive species through cavitation might have degraded the hydrolyzable tannin into soluble substances and gallic acids (Dubey & Tripathy, 2024; Yadav et al., 2021). Furthermore, breakdown of the glucose chain would have occurred, resulting in the conversion of condensed tannin to free tannins, thereby increasing the leaching ability. On the other hand, thermal degradation of phytic acid during US treatment results in the conversion to inositol phosphate with a lower molecular weight (Sarkhel & Roy, 2022). In addition, US pretreatment could have increased the activity of endogenous phytases, which eventually accelerated the hydrolysis of phytic acid and were found to be more effective at the final soaking phase (Yadav et al., 2021). Most importantly, US pretreatment might have induced cleavage formation and destruction of intermolecular hydrogen bonding in phytic acids, resulting in degradation of native structure. Similar kinds of observations (i.e., reduction of tannin and phytic acid) were reported by Yadav et al. (2021) and Dubey and Tripathy (2024) for US-assisted hydration of finger millets. Meanwhile, the reduction of saponin might be attributed to the degradation of glycosidic bonds and the hydrolysis process, which could be accelerated by acoustic cavitation. Additionally, strong shear forces and reactive species (generated during US pretreatment) could have weakened the covalent linkages in carbohydrate and ultimately released the bound saponin (Kheto, Manikpuri, et al., 2024). Then, these compounds were then solubilized with water and leached out through microchannels. However, mechanism behind the reduction of saponin content after US pretreatment was still unclear and needs further investigation. Conclusively, softer cell matrixes and presence of microchannels in US-pretreated GS samples might have increased the leaching ability of ANFs in soaking medium compared to the control. Moreover, increased US amplitude and duration will generate more microchannels by destroying rigid cell matrixes, which ultimately influenced the degradation of ANFs.

3.7. Functional groups

The FTIR spectrum is used to visualize deformation, flexion, and stretching in functional groups. A noticeable change in absorbance pattern of control and US-pretreated GSF was observed within the region of 4000–800 cm^{-1} (Fig. 3A). The 3600–3000 cm^{-1} region showed a wide valley, corresponded to stretching of C–H in terminal alkynes, stretching of O–H in carboxylic acids, stretching of C=O and hydrogen bonding in β-diketones (Silverstein et al., 2005; Zhang et al., 2019). The highest absorbance value was noticed at 3281 cm^{-1}, which gradually declined with increasing amplitude and time. It might be correlated with the weakening of intermolecular hydrogen bonds by US pretreatment. In addition, the reduction of absorbance value in US-pretreated GSF samples suggests hydrogen bonding in secondary amines and stretching of N–H in aliphatic and aromatic primary amines (Silverstein et al., 2005). Cui and Zhu (2020) also reported similar fluctuation in peak intensity

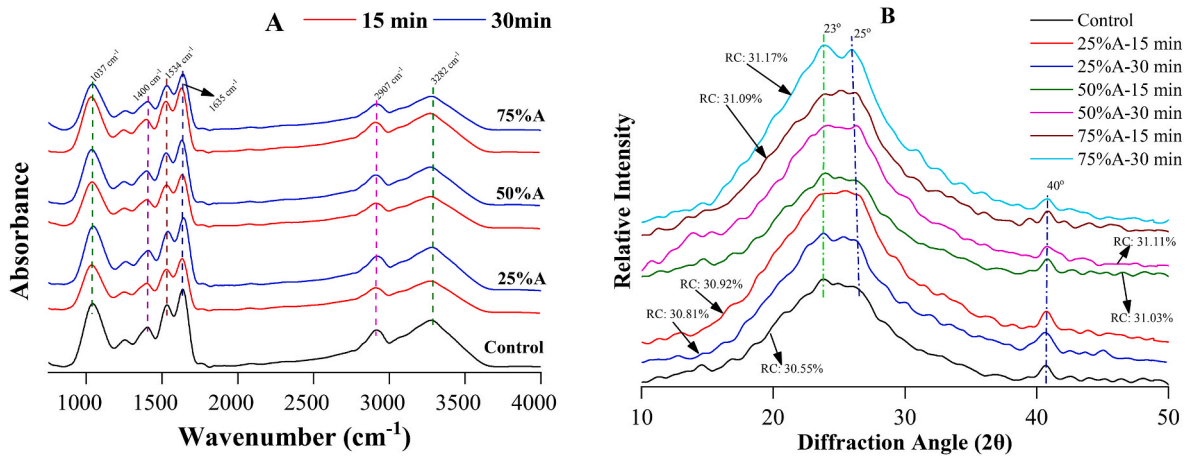

Fig. 3. Effect of US-pretreated soaking on (A) Fourier Transform-Infra Red spectra, and (B) XRD pattern (where RC: Relative crystallinity) of guar seed flour. (For interpretation of the references to color in this figure legend, the reader is referred to the Web version of this article.)

after US treatment of sweet potato and wheat flour. Similarly, the 3600–3000 cm^{-1} region showed a relatively narrow valley, attributed to symmetric and asymmetric stretching of the aliphatic groups (C–H) in lipids and stretching of N–H in primary and secondary amine salts (Silverstein et al., 2005). Like others, absorbance value (highest at 2907 cm^{-1}) varied with treatment conditions, suggesting alternation in –CHO groups. Meanwhile, the 1800–1500 cm^{-1} region corresponded to the polypeptide chain's backbone, indicating structural arrangement/stability of proteins. The highest absorbance value was noticed at 1635 cm^{-1}, attributed to the bending of N–H in Amide II and stronger stretching of C=O and C–O in carboxylic acids. Another one identified at 1534 cm^{-1} had relatively less sharp, attributed to amide I, especially stretching of N–H in primary and secondary amides (Silverstein et al., 2005). Sharp absorbance patterns in US-pretreated samples might be correlated with weaker hydrogen bonding. The strong shear force could degrade the hydrogen bonding during acoustic cavitation, eventually influencing the structural orientation. In addition, Cui and Zhu (2020) claimed that higher peak intensity might be correlated with protein content. Meanwhile, the region of 1450–1200 cm^{-1} had a small valley (with maximum absorbance value at 1400 cm^{-1}) compared to others, which corresponded to the bending of C–H in methyl groups and the presence of diethyl ketone and tertiary alcohols (Silverstein et al., 2005). Furthermore, another board valley was identified at1200–850 cm^{-1}, attributed to stretching of C–C, C–O–H, C–O of the aromatic ring, and C–O–C pyranose ring in carbohydrates, alcohols, and polyphenol (Silverstein et al., 2005). The increase in US amplitude and duration reduced the absorbance value (1037 cm^{-1}), indicating conformational changes in starch granules due to acoustic cavitation (Zhang et al., 2019).

3.8. XRD

The XRD pattern was used to examine the crystalline structure of starch granules, mainly consisting of amylopectin and amylose. As shown in Fig. 3B, the control and US-pretreated GSF samples showed an A-type crystalline pattern with characteristic diffraction peaks at 23 and 25°. Furthermore, a strong diffraction peak was also observed at 40°, indicating a V-type crystalline structure with stronger interactions between starch granules and amino acids (Kheto et al., 2023). The peak intensities of GSF samples varied considerably after US pretreatment. It may be related to the variation in packing density between crystalline and amorphous regions. However, relative crystallinity of GSF samples increased to 31.17 from 30.55%. The US pretreatment could destabilise the crystalline region and then reorganized it again. Furthermore, the increase in relative crystallinity could be attributed to the breakdown of amorphous regions into shorter glucose chains (Estivi et al., 2022). However, break-down of α-1,6-glycosidic bonds and releasing linear glucan can rearrange fragmented chains, resulting in stable double-helix bonds in crystalline regions (Shah et al., 2023). Shah et al. (2023) found similar results with US-treated paddy.

3.9. In-vitro protein digestibility

The *IVPD* of control and US-pretreated soaked GSF was comparable and showed a significant difference ($p < 0.05$) (Fig. 4A). According to our previous studies, soaked GSF samples had better *IVPD* (87.46%) than unsoaked (85.36%) (Kheto et al., 2023). The US-pretreated soaked GSF samples gradually improved the *IVPD* up to 6.75% compared to the control. These phenomena could be attributed to i) cell wall degradation and structural orientation of proteins and ii) leaching of ANFs. Due to acoustic cavitation, US treatment may lead to cleavage formation in polypeptide chains, protein unfolding, and secondary structure modification. The improved unordered structure after US pretreatment indicates that better accessibility of polypeptide chain, as observed in the present study (Aghababaei et al., 2024; Das et al., 2022). Meanwhile, acoustic cavitation could cause disintegration of larger particles into smaller fractions, which eventually increased surface area and ultimately exposed new active binding sites (Aghababaei et al., 2024; Das et al., 2022). Additionally, intermolecular covalent and non-covalent interactions were also disturbed, resulting in higher digestibility (Aghababaei et al., 2024). According to Zhang et al. (2021), intensity and uniformity of the cavitation effect improved as amplitude and time increased. Furthermore, strong microturbulence and shear force generated during US treatment might have weakened the strong interactions of ANFs and other cell wall constituents with proteins (Aghababaei et al., 2024; Kheto, Manikpuri, et al., 2024). As a result, digestible enzymes can easily bind to newly formed active sites, leading to higher *IVPD*.

3.10. Multivariate analysis

The person correlation analysis was used to determine the linear relationship between the variables, as shown in Table 3. TPC and AOA exhibited a significant ($p < 0.01$) positive correlation. Consequently, TPC was the most dominant factor in bioactive compounds. ANFs exhibited a significant ($p < 0.01$) negative correlation with *IVPD*. There was a significant($p < 0.01$) positive correlation between hardness and ANFs. It may be concluded that a harder cell matrix reduces leaching of ANF. WAC and *IVPD* had a significant ($p < 0.01$) positive correlation, suggesting exposure to new active sites. Unfortunately, OAC, WSI, and

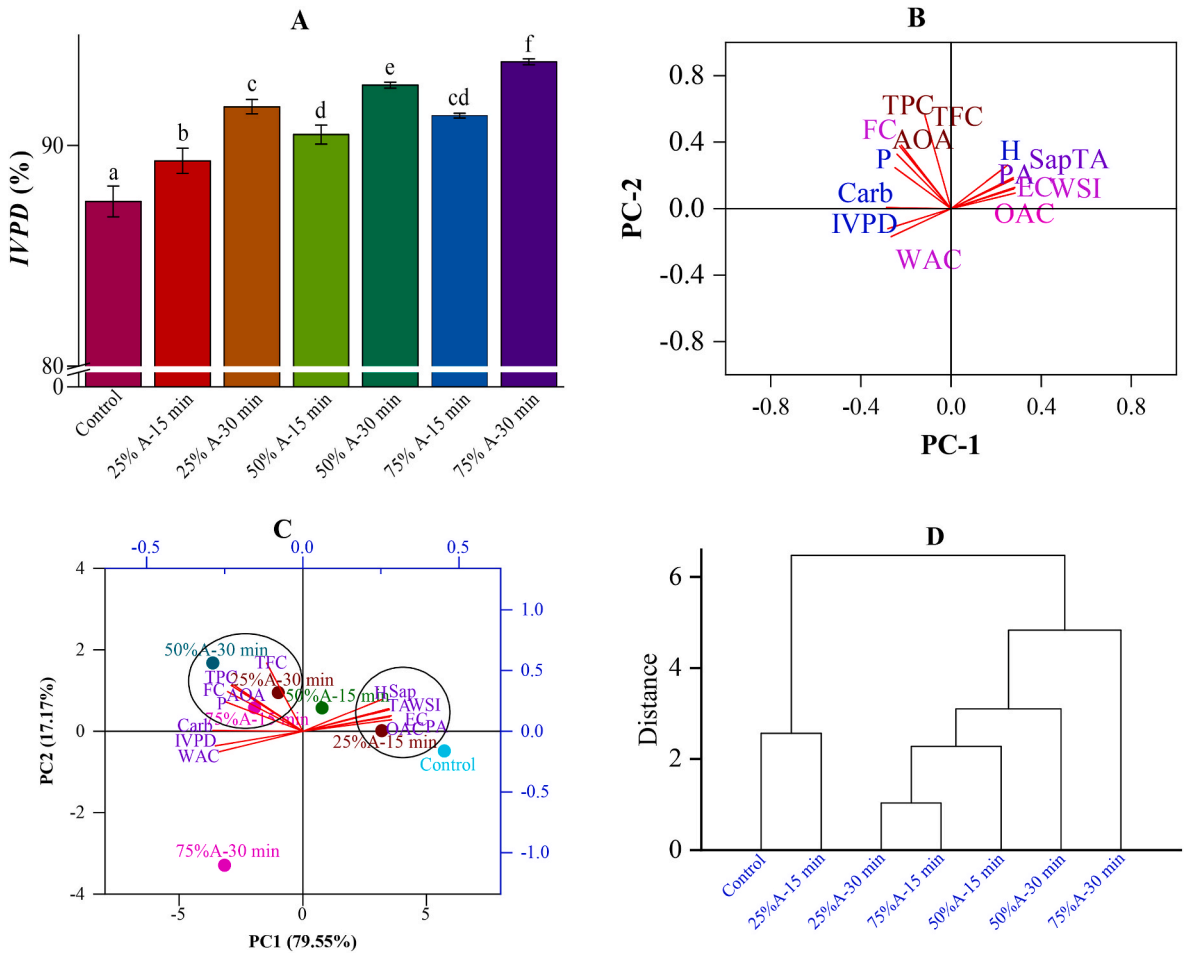

Fig. 4. Effect of US-pretreated soaking on (A) *IVPD:* In-vitro protein digestibility (%), (B) Loading plot & (C) biplot representation from Principal component analysis, and (D) Dendrogram plot form hierarchical cluster analysis of guar seed flour.

EC had a significant ($p < 0.01$) positive correlation with ANFs, which was incorrect. The reduction of ANFs in US-pretreated GSF samples is primarily responsible for the cavitation phenomenon. As a result, it may cause the leaching of water-soluble ANFs and reorganized into a more compact structure.

Therefore, non-linear correlation between the variables was examined through principal component analysis (PCA). The loading plot through PC1 and PC2 shows the distance between different properties from the center point (Fig. 4B). The positive and negative correlations are represented by loading plots that form angles less than 90 and 180° from each other. ANFs exhibited a negative correlation with IVPD, carbohydrate, and bioactive compounds. Meanwhile, protein, foaming capacity, and IVPD were positively correlated. On the other hand, biplot of PCA represents 96.72% of the total variance with scores (treatment conditions) and loading plot (physicochemical properties) (Fig. 4C). Sample treated with 25%A for 15 min formed a cluster with ANFs, hardness, WSI, OAC, and EC. As a result of ANFs and longer soaking duration, low amplitude with a shorter treatment time of US may not be suitable for GS processing. On the other hand, majority of the properties were strongly associated with different treatment conditions (25%A-30 min, 50%A-30 min, and 75%A-15 min). Therefore, identifying the appropriate process parameters became challenging.

To overcome this problem, scores value of PCA were used for hierarchical clustering analysis to determine the Euclidean distance and ward linkage. Like PCA, the physicochemical properties of control and 25%A-15 min treated samples were closely associated in the dendrogram (Fig. 4D). However, the 25%A-30 min and 75%A-15 min treated samples were also closely connected in the dendrogram. According to the findings, low-amplitude US treatment for a longer period requires a longer processing time, which may not be feasible for commercial applications. As a result, 75%A-15 min of US pretreatment may be a better option for shorter soaking time, better *IVPD*, soluble protein, and lower ANFs.

4. Potential applications of ultrasound technology for legumes processing

Previously, we investigated the effect of various processing techniques (such as cold plasma, superheated steam, microwave irradiation, and cold plasma-pretreated germination) on GSF and highlighted both positive and negative aspects (Kheto et al., 2023, 2024a; Manikpuri et al., 2023, 2024). These techniques significantly ($p < 0.05$) reduced ANFs while improving techno-functional properties. However, the taste of bakery items prepared using processed GSF failed to satisfy expectations. Thus, US pretreated soaking process might be useful prior to any further processing. Meanwhile, hard to cook phenomena of legumes can be overcome by US processing.

Since guar germ portions were rich in protein. Soaking is required to separate the endosperm portions prior to protein isolation. As observed in the present investigation, the traditional soaking process required much more time to reach saturated MC. Thus, US pretreatment can reduce the overall processing time for guar germ protein isolation, which was also observed in our recent study of Kheto, Sehrawat, et al. (2024). Several studies claimed that US pretreatment improved protein extraction yields. As per studies, guar germ isolate (91.69%) yield of control sample was 13.33% in alkaline-isoelectric precipitation method

Table 3
Pearson correlation coefficients among different properties of the US-pretreated soaked guar seeds.

	TPC	TFC	AOA	Tannin	Phytic Acid	Saponin	*IVPD*	WAC	OAC	EC	FC	WSI	Protein	Hardness	Carbohydrate
TPC	1														
TFC	0.844[a]	1													
AOA	**0.944**[b]	0.868[a]	1												
Tannin	−0.621	−0.207	−0.647	1											
Phytic Acid	−0.556	−0.128	−0.583	**0.996**[b]	1										
Saponin	−0.544	−0.112	−0.570	**0.993**[b]	**0.996**[b]	1									
IVPD	0.629	0.190	0.640	−0.986[b]	−0.979[b]	−0.983[b]	1								
WAC	0.513	0.155	0.579	−0.952[b]	−0.959[b]	−0.943[b]	**0.912**[b]	1							
OAC	−0.641	−0.183	−0.626	**0.982**[b]	**0.976**[b]	**0.977**[b]	−0.995[b]	−0.893[b]	1						
EC	−0.635	−0.214	−0.636	**0.994**[b]	**0.991**[b]	**0.987**[b]	−0.973[b]	−0.942[b]	**0.977**[b]	1					
FC	**0.987**[b]	0.787[a]	**0.952**[b]	−0.704	−0.645	−0.630	0.718	0.611	−0.723	−0.707	1				
WSI	−0.647	−0.247	−0.687	**0.989**[b]	**0.983**[b]	**0.974**[b]	−0.986[b]	−0.951[b]	**0.977**[b]	**0.974**[b]	−0.741	1			
Protein	0.835[a]	0.694	**0.939**[b]	−0.761[a]	−0.719	−0.696	0.745	0.698	−0.735	−0.739	0.880[b]	−0.803[a]	1		
Hardness	−0.392	−0.016	−0.445	**0.936**[b]	**0.952**[b]	**0.950**[b]	−0.884[b]	−0.963[b]	0.870[a]	**0.937**[b]	−0.476	0.898[b]	−0.576	1	
Carbohydrate	0.751	0.410	0.797[a]	−0.970[b]	−0.946[b]	−0.948[b]	**0.964**[b]	0.899[b]	−0.952[b]	−0.958[b]	0.818[a]	−0.970[b]	0.864[a]	−0.859[a]	1

Where.
[a] $p < 0.05$.
[b] $p < 0.01$.

(Kheto, Sehrawat, et al., 2024). However, the effect on protein extractability in US-pretreated soaked samples, including guar germ proteins, requires further investigation.

5. Conclusion

The present study investigated the effect of US pretreatment with varying amplitude and duration on GS and its physicochemical properties. GS required a longer soaking time due to the presence of galactomannan. Applying US treatment may have promoted the formation of microchannels and weakened intermolecular bonds. As a result, the water absorption rate increased, and the overall soaking time decreased. Like other legumes, the Pelage model was found to be effective in understanding GS hydration. However, the traditional soaking process showed no noticeable reduction of ANFs in GS. Therefore, GS must be pretreated with energy-efficient and sustainable technology, such as US, to reduce ANFs and overall processing time. Most importantly, US-pretreated GS samples showed higher *IVPD* and WAC. Furthermore, US-pretreated soaked GSF may be useful for bakery product formulation or as a partial replacement. Hence, more studies should be carried out using novel technology as a pretreatment method to further shorten the overall soaking time of GS.

CRediT authorship contribution statement

Ankan Kheto: Writing – review & editing, Writing – original draft, Software, Methodology, Investigation, Formal analysis, Data curation, Conceptualization. **Aditi Chaudhari:** Writing – original draft, Formal analysis, Data curation. **Sakshi Manikpuri:** Writing – original draft, Formal analysis, Data curation. **Rachna Sehrawat:** Writing – review & editing, Visualization, Validation, Supervision, Resources, Project administration, Funding acquisition, Conceptualization. **Khalid Gul:** Writing – review & editing, Visualization, Validation. **Lokesh Kumar:** Writing – review & editing, Visualization, Validation, Supervision, Resources, Project administration, Funding acquisition, Conceptualization. **Khursheed Alam Khan:** Writing – review & editing, Visualization, Validation.

Declaration of competing interest

No conflict of interest to declare.

Data availability

Data will be made available on request.

References

Abi-Khattar, A. M., Boussetta, N., Rajha, H. N., Abdel-Massih, R. M., Louka, N., Maroun, R. G., … Debs, E. (2022). Mechanical damage and thermal effect induced by ultrasonic treatment in olive leaf tissue. Impact on polyphenols recovery. *Ultrasonics Sonochemistry, 82*, Article 105895. https://doi.org/10.1016/j.ultsonch.2021.105895

Aghababaei, F., McClement, D. J., & Hadidi, M. (2024). Ultrasound processing for enhanced digestibility of plant proteins. *Food Hydrocolloids, 110188*. https://doi.org/10.1016/j.foodhyd.2024.110188

Aires, M. R., Balbinoti, T. C. V., Maciel, G. M., Fernandes, I. D. A. A., Jorge, R. M. M., & Haminiuk, C. W. I. (2023). Enhancing the parboiling of pantanal rice with ultrasound-assisted hydration: Mass transfer kinetics and bioactive properties. *Journal of Cereal Science, 114*, Article 103762. https://doi.org/10.1016/j.jcs.2023.103762

Chemat, F., Rombaut, N., Sicaire, A. G., Meullemiestre, A., Fabiano-Tixier, A. S., & Abert-Vian, M. (2017). Ultrasound assisted extraction of food and natural products. Mechanisms, techniques, combinations, protocols and applications. A review. *Ultrasonics Sonochemistry, 34*, 540–560. https://doi.org/10.1016/j.ultsonch.2016.06.035

Cui, R., & Zhu, F. (2020). Effect of ultrasound on structural and physicochemical properties of sweet potato and wheat flours. *Ultrasonics Sonochemistry, 66*, Article 105118. https://doi.org/10.1016/j.ultsonch.2020.105118

Das, R. S., Tiwari, B. K., Chemat, F., & Garcia-Vaquero, M. (2022). Impact of ultrasound processing on alternative protein systems: Protein extraction, nutritional effects and

associated challenges. *Ultrasonics Sonochemistry, 91*, Article 106234. https://doi.org/10.1016/j.ultsonch.2022.106234

Dubey, A., & Tripathy, P. P. (2024). Ultrasound-mediated hydration of finger millet: Effects on antinutrients, techno-functional and bioactive properties, with evaluation of ann-PSO and rsm optimization methods. *Food Chemistry, 435*, Article 137516. https://doi.org/10.1016/j.foodchem.2023.137516

Eftekhari, A., Salehi, F., Ardabili, A. G., & Aghajani, N. (2023). Effects of basil seed and guar gums coatings on sensory attributes and quality of dehydrated orange slices using osmotic-ultrasound method. *International Journal of Biological Macromolecules, 253*, Article 127056. https://doi.org/10.1016/j.ijbiomac.2023.127056

Estivi, L., Brandolini, A., Condezo-Hoyos, L., & Hidalgo, A. (2022). Impact of low-frequency ultrasound technology on physical, chemical and technological properties of cereals and pseudocereals. *Ultrasonics Sonochemistry, 86*, Article 106044. https://doi.org/10.1016/j.ultsonch.2022.106044

Kalita, D., Jain, S., Srivastava, B., & Goud, V. V. (2021). Sono-hydro priming process (ultrasound modulated hydration): Modelling hydration kinetic during paddy germination. *Ultrasonics Sonochemistry, 70*, Article 105321. https://doi.org/10.1016/j.ultsonch.2020.105321

Kheto, A., Behera, A., Manikpuri, S., Sehrawat, R., Gul, K., & Kumar, L. (2024). Atmospheric cold plasma pretreatment on germination of guar bean seeds: Effect on germination parameters, bioactive compounds, antinutritional factors, functional groups, and *in vitro* protein digestibility. *Legume Science, 6*(3), e251. https://doi.org/10.1002/leg3.251

Kheto, A., Mallik, A., Sehrawat, R., Gul, K., & Routray, W. (2023). Atmospheric cold plasma induced nutritional & anti-nutritional, molecular modifications and *in-vitro* protein digestibility of guar seed (*Cyamopsis tetragonoloba* L.) flour. *Food Research International, 168*, Article 112790. https://doi.org/10.1016/j.foodres.2023.112790

Kheto, A., Manikpuri, S., Sarkar, A., Das, R., Bebartta, R. P., Kumar, Y., … Sehrawat, R. (2024). How pulse electric field treatment affects anti-nutritional factors and plant protein digestibility: A concise review. *Food Bioscience, 104849*. https://doi.org/10.1016/j.fbio.2024.104849

Kheto, A., Sehrawat, R., Gul, K., & Kumar, L. (2024). Effect of extraction pH on amino acids, nutritional, *in-vitro* protein digestibility, intermolecular interactions, and functional properties of guar germ proteins. *Food Chemistry, 444*, Article 138628. https://doi.org/10.1016/j.foodchem.2024.138628

Kumar, G., Le, D. T., Durco, J., Cianciosi, S., Devkota, L., & Dhital, S. (2023). Innovations in legume processing: Ultrasound-based strategies for enhanced legume hydration and processing. *Trends in Food Science & Technology*. , Article 104122. https://doi.org/10.1016/j.tifs.2023.104122

Lee, C., Kim, E., Kim, H., Heo, W., Ahn, S., Park, J., … Lim, S. (2023). Comparison of the pretreatment methods for enhancing hydration of water-soaked adzuki beans (*Vigna angularis*). *Food Science and Biotechnology*, 1–9. https://doi.org/10.1007/s10068-023-01294-1

Manikpuri, S., Kheto, A., Sehrawat, R., & Gul, K. (2023). How superheated steam treatment modifies the physicochemical, functional, nutritional, and anti-nutritional attributes: A case study on guar bean flour. *Innovative Food Science & Emerging Technologies, 88*, Article 103422. https://doi.org/10.1016/j.ifset.2023.103422

Manikpuri, S., Kheto, A., Sehrawat, R., Gul, K., Routray, W., & Kumar, L. (2024). Microwave irradiation of guar seed flour: Effect on anti-nutritional factors, phytochemicals, *in vitro* protein digestibility, thermo-pasting, structural, and functional attributes. *Journal of Food Science, 89*(4), 2188–2201. https://doi.org/10.1111/1750-3841.16980

Miano, A. C., Ibarz, A., & Augusto, P. E. D. (2017). Ultrasound technology enhances the hydration of corn kernels without affecting their starch properties. *Journal of Food Engineering, 197*, 34–43. https://doi.org/10.1016/j.jfoodeng.2016.10.024

Miano, A. C., Rojas, M. L., & Augusto, P. E. (2019). Using ultrasound for improving hydration and debittering of Andean lupin grains. *Journal of Food Process Engineering, 42*(6), Article e13170. https://doi.org/10.1111/jfpe.13170

Pacheco, F. C., Cunha, J. S., Andressa, I., dos Santos, F. R., Pacheco, A. F. C., Nalon, G. A., … Leite Júnior, B. R. D. C. (2024). Ultrasound-assisted intermittent hydration of pumpkin seeds: Improving the water uptake, germination, and quality of a clean label ingredient. *Food and Bioprocess Technology*, 1–15. https://doi.org/10.1007/s11947-024-03487-w

Patero, T., & Augusto, P. E. (2015). Ultrasound (US) enhances the hydration of sorghum (*Sorghum bicolor*) grains. *Ultrasonics Sonochemistry, 23*, 11–15. https://doi.org/10.1016/j.ultsonch.2014.10.021

Perera, D., Devkota, L., Garnier, G., Panozzo, J., & Dhital, S. (2023). Hard-to-cook phenomenon in common legumes: Chemistry, mechanisms and utilisation. *Food Chemistry, 135743*. https://doi.org/10.1016/j.foodchem.2023.135743

Prajapati, V. D., Jani, G. K., Moradiya, N. G., Randeria, N. P., Nagar, B. J., Naikwadi, N. N., & Variya, B. C. (2013). Galactomannan: A versatile biodegradable seed polysaccharide. *International Journal of Biological Macromolecules, 60*, 83–92. https://doi.org/10.1016/j.ijbiomac.2013.05.017

Pramiu, P. V., Rizzi, R. L., Do Prado, N. V., Coelho, S. R. M., & Bassinello, P. Z. (2015). Numerical modeling of chickpea (*Cicer arietinum*) hydration: The effects of temperature and low pressure. *Journal of Food Engineering, 165*, 112–123. https://doi.org/10.1016/j.jfoodeng.2015.05.020

Salehi, F. (2023). Recent advances in the ultrasound-assisted osmotic dehydration of agricultural products: A review. *Food Bioscience, 51*, Article 102307. https://doi.org/10.1016/j.fbio.2022.102307

Salehi, F., & Inanloodoghouz, M. (2023). Effects of gum-based coatings combined with ultrasonic pretreatment before drying on quality of sour cherries. *Ultrasonics Sonochemistry, 100*, Article 106633. https://doi.org/10.1016/j.ultsonch.2023.106633

Salehi, F., Samary, K., & Tashakori, M. (2024). Influence of organic acids on the viscosity and rheological behavior of guar gum solution. *Results in Engineering, 22*, Article 102307. https://doi.org/10.1016/j.rineng.2024.102307

Sarkhel, S., & Roy, A. (2022). Phytic acid and its reduction in pulse matrix: Structure–function relationship owing to bioavailability enhancement of micronutrients. *Journal of Food Process Engineering*. , Article e14030. https://doi.org/10.1111/jfpe.14030

Shah, A., Wang, Y., Tao, H., Zhang, W., & Cao, S. (2023). Insights into the structural characteristics and *in vitro* starch digestibility on parboiled rice as affected by ultrasound treatment in soaking process. *Food Chemistry X, 19*, Article 100816. https://doi.org/10.1016/j.fochx.2023.100816

Silverstein, R. M., Webster, F. X., & Kiemle, D. J. (2005). Infrared spectroscopy. In D. Brennan, J. Yee, & S. W. Robichaud (Eds.), *Spectrometric identification of organic compounds* (pp. 72–126). New York: John Wiley and Sons.

Yadav, S., Mishra, S., & Pradhan, R. C. (2021). Ultrasound-assisted hydration of finger millet (*Eleusine Coracana*) and its effects on starch isolates and antinutrients. *Ultrasonics Sonochemistry, 73*, Article 105542. https://doi.org/10.1016/j.ultsonch.2021.105542

Yıldırım, A. (2022). Influence of temperature, ultrasound, and variety on moisture diffusivity and thermodynamic properties of some durum wheat varieties during hydration. *Journal of Food Processing and Preservation, 46*(4), Article e16463. https://doi.org/10.1111/jfpp.16463

Zhang, L., Hu, Y., Wang, X., Fakayode, O. A., Ma, H., Zhou, C., … Li, Q. (2021). Improving soaking efficiency of soybeans through sweeping frequency ultrasound assisted by parameters optimization. *Ultrasonics Sonochemistry, 79*, Article 105794. https://doi.org/10.1016/j.ultsonch.2021.105794

Zhang, Y., Wang, B., Zhang, W., Xu, W., & Hu, Z. (2019). Effects and mechanism of dilute acid soaking with ultrasound pretreatment on rice bran protein extraction. *Journal of Cereal Science, 87*, 318–324. https://doi.org/10.1016/j.jcs.2019.04.018